Dalton Transactions

ROYAL SOCIETY OF CHEMISTRY

PAPER

View Article Online
View Journal | View Issue

Cite this: *Dalton Trans.*, 2023, **52**, 12779

Synthesis and catalytic activity of well-defined Co(I) complexes based on NHC–phosphane pincer ligands†

Ana Luque-Gómez, Pilar García-Orduña, Fernando J. Lahoz and Manuel Iglesias *

Received 13th February 2023,
Accepted 8th August 2023

DOI: 10.1039/d3dt00463e

rsc.li/dalton

A new methodology for the preparation of Co(I)–NHC (NHC = N-heterocyclic carbene) complexes, namely, $[Co(PC^{NHC}P)(CO)_2][Co(CO)_4]$ (**1**) and $[Co(PC^{NHC}P)(CO)_2]BF_4$ (**2**), has been developed ($PC^{NHC}P$ = 1,3-bis(2-(diphenylphosphanyl)ethyl)-imidazol-2-ylidene). Both complexes can be straightforwardly prepared by direct reaction of their parent imidazolium salts with the Co(0) complex $Co_2(CO)_8$. Complex **1** efficiently catalyses the reductive amination of furfural and levulinic acid employing silanes as reducing agents under mild conditions. Furfural has been converted into a variety of secondary and tertiary amines employing dimethyl carbonate as the solvent, while levulinic acid has been converted into pyrrolidines under solventless conditions. Dehydrocoupling of the silane to give polysilanes has been observed to occur as a side reaction of the hydrosilylation process.

Introduction

The switch from petrochemicals to renewable bio-based products is pivotal for successful transition towards a circular economy.[1] However, the transformation of biomass feedstocks into value-added products also requires the development of sustainable processes that avoid the generation of waste and the use of energy-extensive and cost-ineffective reactions.[2] In this regard, catalysis is at the core of modern chemical synthesis, being a fundamental pillar of green and sustainable chemistry.[3]

Earth-abundant metals (EAMs), compared to platinum group metals (PGMs), are readily available and inexpensive, and usually have a relatively lower environmental impact. In consequence, the development of homogeneous catalysts based on EAMs has undergone remarkable revitalization over the last decade.[4] Among them, cobalt catalysts have shown excellent performances in a broad variety of reactions,[5] for example, in the reduction of organic substrates *via* hydrogenation,[6] transfer hydrogenation,[7] hydrosilylation,[8,9] reductive amination[10] or hydroboration.[11]

Co(I) complexes have often been proposed as the active species in cobalt-catalysed processes;[12,11b] however, convenient synthetic methods for the preparation of well-defined Co(I) complexes are scarce.[13] In particular, the synthesis of NHC–Co(I) complexes (NHC = N-heterocyclic carbene) has been described by the reaction of the free NHC ligand with $[Co(PPh_3)_3Cl]$,[14] by the reduction of NHC–Co(II) complexes,[15] or by the oxidation of NHC–Co(0) complexes with 2,2,6,6-tetramethylpiperidine-1-oxyl (TEMPO).[16] The limitations of these synthetic methodologies have hampered the preparation of NHC–Co(I) organometallic complexes, which are promising homogeneous catalysts owing to the unique properties of NHCs and their success story as ancillary ligands in catalysis.[17]

Levulinic acid (LA) and furanics are key bio-based building blocks that can be easily obtained from the hexoses in lignocellulosic biomass.[18] The catalytic reductive amination reaction shows promise as a sustainable method for the functionalization of biomass, which allows the synthesis of amines directly from carbonyl compounds (ketones, aldehydes or carboxylic acids).[19] However, examples of the cobalt-catalyzed reductive amination of carbonyl compounds employing hydrosilanes as reducing agents are scarce.[10] In fact, homogeneous cobalt catalysts have been extensively explored in the hydrosilylation of alkenes, alkynes and, to a lesser extent, carbonyl compounds;[9] however, imines have been widely overlooked.[20] An interesting example of the reductive amination of carbonyl compounds promoted by homogeneous cobalt catalysts has been reported by Beller and Jagadeesh.[10c]

The valorisation of levulinic acid *via* reductive amination may afford pyrrolidinones or pyrrolidines by the ensuing reduction of the carbonyl group. Most of the homogeneous catalysts reported for these transformations are based on PGMs.[21] The only examples of EAM catalysts for the preparation of pyrrolidines are complexes $[Fe(Cp^*)(IMes)(CO)_2]I$ and $[Fe(IMes)(CO)_4]$ (Cp^* = 1,2,3,4,5-pentamethylcyclopentadiene;

Instituto de Síntesis Química y Catálisis Homogénea (ISQCH), CSIC-Universidad de Zaragoza, C/Pedro Cerbuna 12, 50009-Zaragoza, Spain. E-mail: miglesia@unizar.es

†Electronic supplementary information (ESI) available. CCDC 2279813 for (**1**). See DOI: https://doi.org/10.1039/d3dt00463e

IMes = 1,3-bis(2,4,6-trimethylphenyl)imidazol-2-ylidene), which operate in the presence of 6 equiv. of $PhSiH_3$ and visible light irradiation at 100 °C.[22] In this regard, it is worth mentioning that the *N*-alkylation of a variety of carboxylic acids—including LA—with silanes as reducing agents and $B(C_6F_5)_3$ as a catalyst has been also described.[23]

We envisaged that the use of a PCP ligand containing a central NHC moiety ($PC^{NHC}P$), recently employed by us for the synthesis of Ir(I) complexes,[24] would provide an interesting new class of stable, well-defined NHC–Co(I) catalysts. The novel Co(I) complexes prepared herein were studied as catalysts for the reductive amination of bio-based platform chemicals, namely, furfural and levulinic acid.

Results and discussion

Synthetic procedures *via* free-NHC or transmetallation from silver–NHC complexes proved to be unsuccessful for the synthesis of cobalt(I) complexes with our $PC^{NHC}P$ ligand. Therefore, we explored the direct reaction of the parent imidazolium salt **$PC^{NHC}P$·HX** (X = Cl or BF_4) with 0.5 equiv. of $[Co_2(CO)_8]$. We reasoned that oxidative addition of the C_2–H bond of the imidazolium salt would afford a transient $PC^{NHC}P$–Co(II) hydride, which upon release of 0.5 equiv. of H_2 would render the desired $PC^{NHC}P$–Co(I) complex, analogously to the reductions of Co(II) halides with $K(HBEt_3)$ as reported by Gomes and co-workers.[25]

Both imidazolium salts, **$PC^{NHC}P$·HX** (X = Cl or BF_4), were initially reacted with 0.5 equiv. of $[Co_2(CO)_8]$ in THF at room temperature (Scheme 1). The reactions were monitored by ^{31}P NMR spectroscopy, showing complete consumption of **$PC^{NHC}P$·HCl** and intermediate species after 24 h. In contrast, in the case of the BF_4 salt, the crude product needs to be refluxed in acetonitrile for the peaks of the intermediates to disappear in the ^{31}P NMR spectrum. To our surprise, in the case of **$PC^{NHC}P$·HCl**, the Co(I)/Co(–I) complex $[Co(\kappa^3\text{-}P,C,P'\text{-}PC^{NHC}P)(CO)_2][Co(CO)_4]$ (**1**) was obtained, while the reaction with the BF_4 salt afforded the Co(I) complex $[Co(\kappa^3\text{-}P,C,P'\text{-}PC^{NHC}P)(CO)_2]BF_4$ (**2**).

The gradual diffusion of hexane into a solution containing complex **1** in THF allowed us to obtain crystals suitable for single-crystal X-ray diffraction. The cation displays a slightly distorted trigonal bipyramidal geometry with the $\kappa^3\text{-}P,C,P'\text{-}PC^{NHC}P$ ligand showing a *mer* coordination with a P(1)–Co(1)–P(2) angle of 165.820(19)°. The two phosphane moieties are situated at the axial positions, while the NHC and carbonyl ligands occupy the equatorial plane. The NHC ring N(1)–C(1)–N(2)–C(17)–C(16) forms an angle of 39.46(7)° with the equatorial plane Co(1)–C(1)–C(33)–C(32), which situates the wingtip groups above and below the NHC plane. Both six-membered chelate rings, C(1)–Co(1)–P(2)–C(19)–C(18)–N(2) and C(1)–Co(1)–P(1)–C(14)–C(15)–N(1), present a highly deviated from planarity $^{1,4}B$ boat conformation (Fig. 1).[26]

Complexes **1** and **2** are both diamagnetic, which allowed full characterisation by NMR spectroscopy.

The ^1H NMR spectrum of **1** shows the disappearance of the resonance that corresponds to imidazolium's C_2 proton and the emergence of two multiplets at δ 4.26–4.11 and 3.05–2.93 ppm that correspond to the methylenic protons of the NCH_2 and PCH_2 moieties, respectively. The $^{13}C\{^1H\}$ NMR spectrum of **1** confirms the $\kappa^3\text{-}P,C,P'$ coordination of the $PC^{NHC}P$ ligand to the cobalt centre, as well as the presence of a carbonyl ligand. The carbene carbon shows a triplet at δ 174.0 ppm ($^2J_{CP}$ = 38.1 Hz) due to the coupling with the two ^{31}P nuclei of the wingtip groups. The CO ligands also appear as a triplet at δ 198.6 ppm ($^2J_{CP}$ = 23.6 Hz). The $^{31}P\{^1H\}$ NMR features a singlet resonance at δ 59.1 ppm, thus suggesting the presence of a symmetry plane that renders both P nuclei equivalent.

In order to gain mechanistic insight into the formation of **1**, we monitored the reaction of **$PC^{NHC}P$·HCl** with 0.5 equiv. of

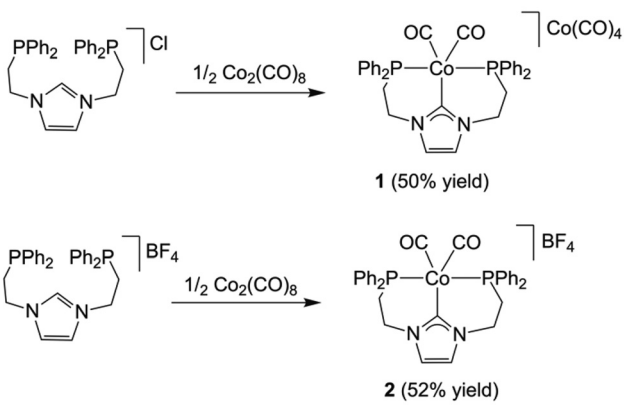

Scheme 1 Synthetic route for the preparation of **1** and **2**. Reaction conditions: X = Cl: THF, room temperature, 1 d. X = BF_4: THF, room temperature, 1 d; followed by CH_3CN, 80 °C, 3 d.

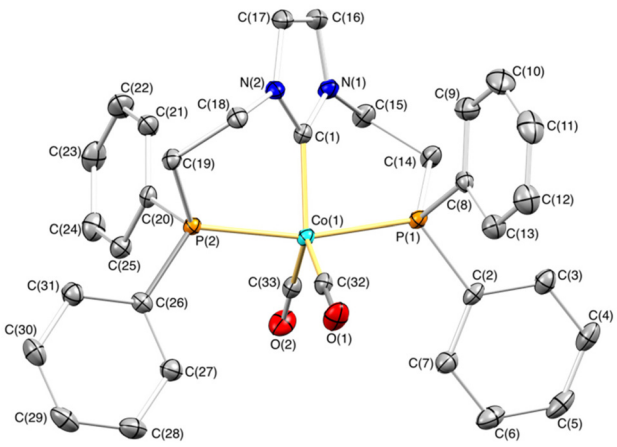

Fig. 1 Molecular structure of cationic complex **1**. Hydrogen atoms, solvent molecules and the $[Co(CO)_4]^-$ counterion were omitted for clarity. Selected bond lengths (Å) and angles (°): Co(1)–P(1) 2.1868(5), Co(1)–P(2) 2.1796(5), Co(1)–C(1) 1.9502(17), Co(1)–C(32) 1.7724(18), Co(1)–C(33) 1.7738(18), P(1)–Co(1)–C(32) 92.11(6), P(1)–Co(1)–C(33) 95.45(5), P(2)–Co(1)–C(1) 82.78(5), P(2)–Co(1)–C(32) 94.21(6), P(2)–Co(1)–C(33) 92.83(5), P(1)–Co(1)–P(2) 165.820(19), C(1)–Co(1)–C(32) 121.56(7), P(1)–Co(1)–C(1) 83.09(5), C(1)–Co(1)–C(33) 120.78(8).

$Co_2(CO)_8$ in THF-d_8 at 298 K by $^{31}P\{^1H\}$ NMR (Fig. 2). After 1 h, the $^{31}P\{^1H\}$ NMR spectrum shows a broad singlet at *ca.* δ −19 ppm, and two broad multiplets between δ 45 and 57 ppm. At this point, also the incipient formation of **1** is observed as a sharp singlet at δ 59.2 ppm. The broad resonances suggest that, initially, a mixture of complexes in equilibrium with each other is formed. These initial species can be assigned to a Co(I)/Co(−I) dinuclear complex ($[Co(\kappa^2\text{-}P,P'\text{-}PC^{NHC}P{\cdot}HCl)(CO)_n]_2$) or a $[Co(\kappa^2\text{-}P,P'\text{-}PC^{NHC}P{\cdot}HCl)_2][Co(CO)_4]$ cationic complex.[27] Subsequently, these species plausibly evolve to give the Co(I)/Co(−I) complex **1** and paramagnetic Co species.

The ^1H, $^{13}C\{^1H\}$ and $^{31}P\{^1H\}$ NMR spectra of **2** in CD_3CN show no remarkable differences compared with those described above for **1**.

High-resolution electrospray ionization mass spectrometry (HR-ESI-MS) of **1** and **2** shows the cations $[Co(PC^{NHC}P)(CO)]^+$ and $[Co(PC^{NHC}P)]^+$ as main species. The FT-IR spectrum of **1** shows two strong bands at 1991 and 1935 cm^{-1}, which are consistent with the presence of two CO ligands,[28] and an intense band at 1882 cm^{-1} that can be attributed to the $[Co(CO)_4]^-$ anion.[13] In contrast, complex **2** shows only two strong bands at 1989 and 1930 cm^{-1} that correspond to the two carbonyl ligands of the Co(I) cation (Fig. 3). The presence of the BF_4^- counterion is further supported by a broad band at 1000–1100 cm^{-1} in the FTIR spectrum and a resonance at δ −151.2 ppm in the ^{19}F NMR spectrum.

Conductometric determinations of solutions of **1** and **2** in CH_3CN (5×10^{-4} M) at room temperature revealed molar conductivities of 45 and 50 S mol^{-1} cm^{-1}, respectively, which are compatible with a 1 : 1 electrolyte.

The lability of the second carbonyl ligand has been reported for related complexes,[28a,29] which may lead to the formation of an unsaturated species under catalytic conditions.

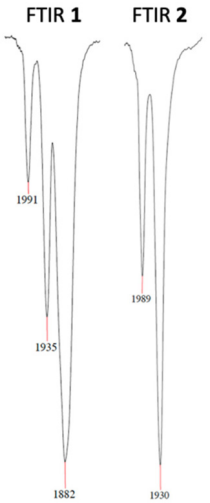

Fig. 3 ν(CO) vibration bands in the FTIR spectra of complexes **1** and **2**.

In order to explore the catalytic activity of complexes **1** and **2**, initially, they were tested as catalysts in the reductive amination of furfural (FAL). The reaction was performed in dimethylcarbonate (DMC), which is considered a green solvent, mainly due to its low volatility, good biodegradability and low toxicity (Scheme 2 and Table 1).[30] The one-pot reaction of *p*-toluidine with FAL with $PhSiH_3$ as the reducing agent and 5 mol% of **1** (entry 1) at 80 °C led to an 88% yield of silylamine. The yield was improved by using a sequential process that entails the reaction of *p*-toluidine with FAL in the presence of **1** (5 mol%) for 1 h at 80 °C followed by the addition of $PhSiH_3$ (entry 2). It must be noted that the use of $PhSiH_3$ leads to the formation of a mixture of aminosilanes, diaminosilanes, and oligomers, except in the case of secondary amines.

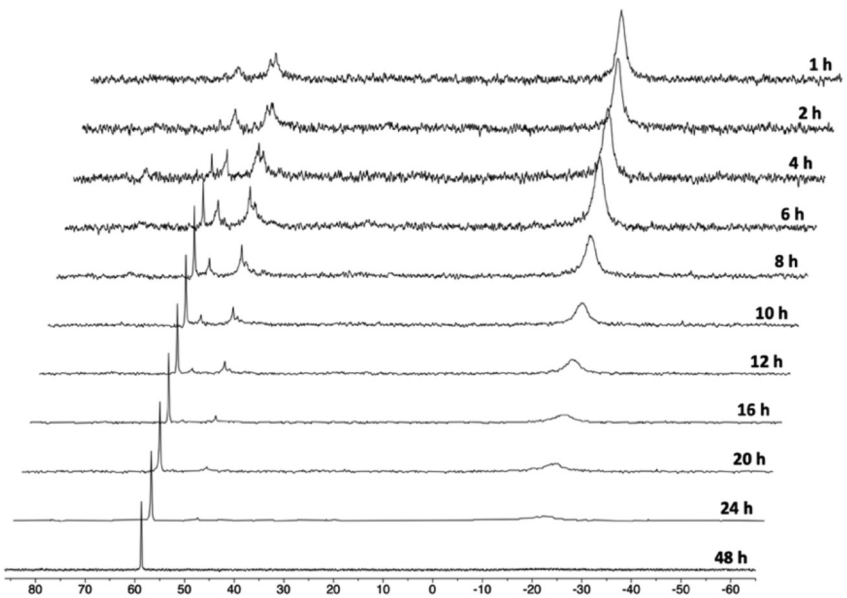

Fig. 2 $^{31}P\{^1H\}$ NMR monitoring of the formation of **1**.

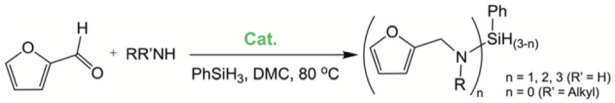

Scheme 2 Reductive amination of furfural in DMC employing $PhSiH_3$ as a reducing agent.

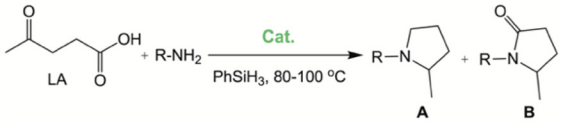

Scheme 3 Solventless reductive amination of levulinic acid to pyrrolidine or pyrrolidinone with $PhSiH_3$ as a reducing agent.

Table 1 Reductive amination of furfural in DMC[a]

Entry	Amine	Time (h)	Conversion[e] (%)
1[b]	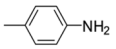	23	88
2	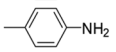	20	>99
3[c]	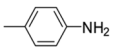	20	53
4[d]	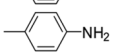	20	56
5	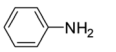	20	82
6	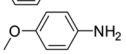	20	80
7	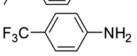	20	64
8	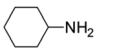	20	50
9	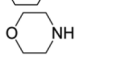	20	73

[a] Reaction conditions: 0.125 mmol of amine, 0.125 mmol of furfural and 0.25 mmol of $PhSiH_3$, 5 mol% of **1**, at 80 °C in DMC. [b] One pot reaction. [c] 5 mol% of **2**. [d] 1 mol% of **1**. [e] Conversions were determined by ^1H NMR spectroscopy of the crude material.

Under analogous conditions, catalyst **2** leads to a noticeably lower yield (entry 3). The higher activity of **1** can be ascribed to the presence of the $Co(CO)_4^-$ counterion since this is the only structural difference between both complexes. A decrease in the loading of **1** to 1 mol% also results in a significant drop in the catalytic activity (entry 4). Therefore, other amines were also tested under the conditions described above for entry 2. The use of aniline or *p*-anisidine results in yields of *ca.* 80% (entries 5 and 6), while in the case of 4-(trifluoromethyl) aniline, the yield drops to 64% (entry 7). Longer reaction times for the formation of the imine led to similar yields. Cyclohexylamine was explored as a substrate in order to expand the scope of the reaction to aliphatic amines, resulting in a 50% yield (entry 8). It is noteworthy that secondary aliphatic amines readily react under analogous conditions to afford the corresponding tertiary amines in good yields (entry 9). In order to probe the synthetic utility of this methodology, the reaction of furfural with *p*-toluidine (under conditions analogous to those described in entry 2, Table 1) was scaled up to 2 mmol of the substrate. After purification, a 79% yield was obtained for the synthesis of *N*-(furan-2-ylmethyl)-4-methylaniline.

The results described above and the dearth of suitable EAM catalysts for the synthesis of pyrrolidines by reductive amination of LA prompted us to study the catalytic activity of complexes **1** and **2** in these reactions (Scheme 3). The optimization of reaction conditions was explored by employing *p*-toluidine under solventless conditions and **1** as the catalyst. First, reaction conditions similar to those reported by Darcel and coworkers were used,[22] *i.e.*, 6 equiv. of $PhSiH_3$, 5 mol% of **1**, 100 °C for 20 h; however, in our case, visible light irradiation was not required. Quantitative formation of the corresponding pyrrolidine was observed, which prompted us to evaluate the activity of **1** under milder conditions. Quantitative yields of pyrrolidine (**A**) were also obtained at shorter reaction times, namely, after 5 h (Table 2; entry 1). The reduction of the amount of $PhSiH_3$ to 2 equiv. also leads to the exclusive formation of **A** in quantitative yields at 80 °C (Table 2; entry 2). It is worth mentioning that, under analogous conditions, the use of **2** as a catalyst leads to a 42% yield, which is consistent with the reactivity trend described previously for the reductive amination of furfural. Finally, we evaluated the influence of catalyst loading. The use of 1 mol% of **1** also allows quantitative yields of **A** at 80 °C in 5 h, but 6 equiv. of $PhSiH_3$ is required (Table 2; entry 3). Under these conditions, 4-methoxyaniline also brings about quantitative yields (Table 2; entry 4). However, aniline gives rise to lower conversions and selectivities (Table 2; entry 5), but total conversion was achieved by increasing the reaction time to 20 h (Table 2; entry 6). The presence of an electron-attracting group in aniline, such as CF_3, results in a significant drop in the catalytic activity in the case of 4-trifluoromethylaniline (Table 2; entry 7). In this case, a mixture of **A**, **B** and other reaction intermediates is observed after 20 h at 100 °C. The reaction was scaled up to 1.35 mmol of levulinic acid to probe the synthetic value of this reaction, employing 1 equivalent of *p*-toluidine (under conditions analogous to those described in entry 1, Table 2), leading to an 87% yield of 2-methyl-1-(*p*-tolyl)pyrrolidine after purification.

To explore the stability of the catalyst (**1**), the crude mixtures of all the catalytic experiments were studied by $^{31}P\{^1H\}$ NMR spectroscopy at the end of the reaction, showing exclusively one peak at δ 59.2 ppm in all cases, which corresponds to the shift observed for **1** in acetonitrile. However, this resonance could be attributed to the presence of an unreacted catalyst at the end of the reaction. Consequently, stoichiometric experiments between **1** and $PhSiH_3$ were carried out in a Young NMR tube to shed light on the nature of the active species. Complex **1** was reacted with 2 equivalents of $PhSiH_3$ in THF-d_8, showing moderate gas evolution at 60 °C. After 24 h at 60 °C, the $^{31}P\{^1H\}$ NMR spectrum (Fig. S32†) shows the peak characteristic of **1** at δ 59.2 ppm, together with two broad peaks in a 1 : 1 ratio at δ 36.2 and 33.2 ppm, as the main

Table 2 Solventless reductive amination of levulinic acid[a]

Entry	Amine	Equiv. $PhSiH_3$	Loading (mol %)	T (°C)	Time (h)	Conversion % (A/B ratio)[b]
1	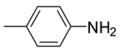	6	5	100	5	>99 (100/0)
2	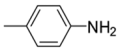	2	5	80	5	>99 (100/0)
3	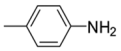	6	1	80	5	>99 (100/0)
4	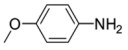	6	1	80	5	>99 (100/0)
5		6	1	80	5	83 (70/30)
6		6	1	80	20	>99 (100/0)
7	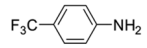	6	5	100	20	12 (—)

[a] Reaction conditions: 0.25 mmol of levulinic acid, 0.25 mmol of amine, 1 mol% of **1**, at 80 °C neat. [b] Conversions were determined by ^{1}H NMR spectroscopy of the crude material.

species in solution. These two resonances plausibly correspond to a complex where the $PC^{NHC}P$ ligand adopts a facial geometry,[31] which makes both phosphorous nuclei inequivalent.[32] A sharp singlet at δ 26.2 ppm and a broad multiplet at δ −20.3 ppm are also observed as minor products. The ^{1}H NMR spectrum shows no hydride peak attributable to the oxidative addition of the Si–H bond, but it confirms the presence of **1** accompanied by a mixture of other diamagnetic species. Remarkably, a sharp singlet due to H_2 formation appears at δ 4.57 ppm, which suggests that acceptorless dehydrogenative coupling of the silane is taking place (Fig. S33†).[33] This reactivity agrees with the fact that the ^{1}H NMR spectra of the catalytic reactions show the formation of polysilanes *via* dehydrocoupling of $PhSiH_3$. This was confirmed by the ^{19}Si–^{1}H HMBC spectrum of the reaction mixture of the reductive amination of levulinic acid with *p*-toluidine (Table 2, entry 3), which shows a correlation between the resonances at 5.37–5.21 in the ^{1}H NMR spectrum and a peak at *ca.* δ −28 ppm in the ^{19}Si NMR spectrum (Fig. S36†). The ^{29}Si DEPT spectrum shows two groups of resonances, from δ −20 to −29 ppm and from δ −40 to −52 ppm, that correspond to the different dehydrocoupling products formed as a by-product of the hydrosilylation reaction (Fig. S37†). Moreover, it is noteworthy that a white precipitate, attributable to the formation of a polymer, forms at long reaction times. An analogous experiment was performed in CD_3CN at 80 °C, showing comparable results. However, in this case, the ^{1}H and $^{31}P\{^1H\}$ NMR spectra show **1** as the main species throughout the reaction, which allows the sharp singlet of H_2 at δ 4.55 ppm to be observed in a cleaner region (Fig. S34 and S35†). Homogeneous catalysts based on other metal centres have been reported for the dehydrocoupling of $PhSiH_3$ to give polysilanes;[34] however, to the best of our knowledge, this is the first example of a cobalt catalyst for this transformation.

Hydride resonances are not observed by ^{1}H NMR spectroscopy, but it is conceivable that transient hydride species are formed during the reaction. In this regard, the most widely accepted mechanism for the dehydrocoupling of $PhSiH_3$ has been reported to require the formation of a metal hydride, which reacts with the silane *via* σ-bond metathesis to give the silyl intermediate and H_2. Subsequently, Si–Si bond formation occurs by reaction of the silyl intermediate with a new molecule of silane, again *via* a σ-bond metathesis step.[35] However, it must be noted that this mechanism has been proposed for Ti and Zr catalysts.

Ionic outer-sphere mechanisms are frequently observed in silane-mediated reductions and do not entail the oxidative addition of the Si–H bond. Consequently, it can be postulated that the aforementioned reactions may proceed *via* this class of mechanisms. The seminal work on these types of mechanisms by Piers,[36] Brookhart[37] and Bullock[38] has triggered the development of a myriad of new hydrosilylation catalysts. Noteworthy precedents of this type of catalyst have been reported by the groups of Brookhart,[39] Nikonov,[40] Oestreich[41] and others.[42] A tentative reaction mechanism for the hydrosilylation of imines with **1** would entail the end-on coordination of $PhSiH_3$ to the cation $[Co(\kappa^3\text{-}P,C,P'\text{-}PC^{NHC}P)(CO)]^+$, followed by heterolytic splitting of the Si–H bond assisted by the imine or the $[Co(CO)_4]^-$ ion. Bifunctional catalysts based on the Lewis base characteristics of the latter have been reported; namely, the cooperative ring opening of epoxides by a Lewis acid metal centre and a $[Co(CO)_4]^-$ counterion acting as a Lewis base has been proposed as a key step in epoxide functionalization.[43] The heterolytic splitting of the Si–H bond results in the formation of a Co-hydride species and a silyl iminium cation, either directly or *via* a $[Co(CO)_4]^-$ shuttle. Finally, hydride transfer furnishes the hydrosilylation product, regenerating the active species. However, detailed mechanistic studies are required to confirm this postulation.

Conclusions

In summary, we have developed a new methodology for the preparation of NHC–Co(I) complexes directly from their parent imidazolium salts. Remarkably, the nature of the counterion

of the imidazolium salt plays an important role in the selectivity of the reaction, with $PC^{NHC}P{\cdot}HCl$ affording the Co(I)/Co(−I) complex $[Co(\kappa^3\text{-}P,C,P'\text{-}PC^{NHC}P)(CO)_2][Co(CO)_4]$ (**1**), and $PC^{NHC}P{\cdot}HBF_4$ affording the Co(I) complex $[Co(\kappa^3\text{-}P,C,P'\text{-}PC^{NHC}P)(CO)_2]BF_4$ (**2**). Complex **1** shows promise as a catalyst for reductive amination reactions employing $PhSiH_3$ as a reducing agent; however, the use of **2** results in markedly worse performances under analogous conditions. The higher activity of **1** seems to be originated by the presence of the $[Co(CO)_4]^-$ counterion. Furfural was converted into a variety of secondary and tertiary amines, in DMC, by reaction with aromatic and aliphatic primary amines, and aliphatic secondary amines. Moreover, levulinic acid was converted into pyrrolidines under mild, solventless conditions using a 1 mol% loading of **1**, this being the first example of a cobalt complex to catalyse this transformation. Moreover, it is remarkable that **1** also catalyses the dehydrocoupling of $PhSiH_3$, with polysilanes being observed as reaction by-products. Finally, we believe that the synthetic methodology described here provides useful information for the preparation of novel, well-defined NHC–Co(I) catalysts.

Experimental

General methods

All experiments and manipulations were carried out under an argon atmosphere using standard Schlenk techniques or in an argon-filled glove box. The solvents were dried by known procedures and distilled under argon prior to use or obtained oxygen- and water-free from a solvent purification system (Innovative Technologies). Deuterated solvents were dried over molecular sieves or calcium hydride (THF-d_8, $CDCl_3$ and CD_3CN). All other commercially available starting materials were used without further purification. ^1H, $^{13}C\{^1H\}$, $^{31}P\{^1H\}$ and ^{19}F spectra were recorded either on a Bruker ARX 300 MHz or a Bruker Avance 400 MHz instrument. Chemical shifts (expressed in parts per million) are referenced to residual solvent peaks (^1H, $^{13}C\{^1H\}$). Coupling constants, *J*, are given in Hz. Spectral assignments were achieved by a combination of ^1H–^1H COSY, ^{13}C APT and ^1H–^{13}C HSQC/HMBC experiments. High-resolution electrospray mass spectra (HRMS) were acquired using a MicroTOF-Q hybrid quadrupole time-of-flight spectrometer (Bruker Daltonics, Bremen, Germany). Attenuated total reflection infrared spectra (ATR-IR) of solid samples were recorded on a PerkinElmer Spectrum 100 FT-IR spectrometer.

Synthesis of $[Co(PC^{NHC}P)(CO)_2][Co(CO)_4]$ (1). $Co_2(CO)_8$ (48.5 mg, 0.142 mmol) and $PC^{NHC}P{\cdot}HCl$ (150 mg, 0.284 mmol) were weighed inside a glovebox and placed in a Schlenk flask. Subsequently, both solids were dissolved in 25 mL of THF, and the resulting reaction mixture was stirred at r.t. for 24 h in a Schlenk flask equipped with a bubbler inside a well-ventilated fume hood in order to allow the release of the gases formed during the reaction (CO and H_2). Sometimes a green precipitate appears after stirring in THF for 24 h. This precipitate can be dissolved in CH_3CN at 70 °C to afford a new batch of **1**. Filtration of the solution followed by evaporation of the solvent afforded a green residue that was washed with pentane (3 × 12 mL). After filtration through a short pad of neutral alumina, complex **1** was isolated as a yellow microcrystalline solid in 50% yield (55 mg, 0.71 mmol). ^1H NMR (CD_3CN, 400 MHz): δ 7.58–7.20 (m, 10H, CH_{Ar} + 2H, CH_{im}), 4.26–4.11 (m, 4H, NCH_2), 3.05–2.93 (m, 4H, PCH_2). $^{13}C\{^1H\}$ NMR (CD_3CN, 175 MHz): δ 198.6 (t, $^2J_{CP}$ = 23.6, *C*O), 174.0 (t, $^2J_{CP}$ = 38.1, *NC*N), 134.8 (app. t, $^1J_{C-P}$ = 24.5, C_{ipso}), 131.6 (app. t, $^2J_{C-P}$ = 5.2, CH_{orto}), 131.2 (s, CH_{para}), 129.1 (app. t, $^3J_{C-P}$ = 5.2, CH_{meta}), 123.6 (s, CH_{im}), 47.6 (s, NCH_2), 30.3 (t, $^1J_{C-P}$ = 19.5, NCH_2). $^{31}P\{^1H\}$ NMR (CD_3CN, 121 MHz): δ 59.1 (s, PPh_2). IR (cm^{-1}, pure sample): 1933, 1865 cm^{-1}. HRMS (ESI+): *m*/*z* Calcd for $C_{32}H_{30}N_2OP_2CoCl$: (M–CO–Cl^-): 579.1144, Exp: 579.1165.

Synthesis of $[Co(PC^{NHC}P)(CO)_2][BF_4]$ (2). $Co_2(CO)_8$ (41.3 mg, 0.121 mmol) and $PC^{NHC}P{\cdot}HBF_4$ (140 mg, 0.241 mmol) were weighed inside a glovebox and placed in a Schlenk flask. Subsequently, both solids were dissolved in 25 mL of THF, and the resulting reaction mixture was stirred at r.t. for 24 h in a Schlenk flask equipped with a bubbler inside a well-ventilated fume hood in order to allow the release of the gases formed during the reaction (CO and H_2). Then, the solvent was evaporated, 10 mL of CH_3CN was added and the solution thus obtained was stirred at 80 °C for 3 d. Evaporation of the solvent afforded a green residue that was washed with pentane (3 × 12 mL). After filtration through a short pad of neutral alumina, complex **2** was isolated as a yellow microcrystalline solid in 52% yield (87 mg, 0.125 mmol). ^1H NMR (CD_3CN, 400 MHz): δ 7.85–7.11 (m, 10H, CH_{Ar} + 2H, CH_{im}), 4.29–4.12 (m, 4H, NCH_2), 3.12–2.96 (m, 4H, PCH_2). $^{13}C\{^1H\}$ NMR (CD_3CN, 175 MHz): δ 198.6 (t, $^2J_{CP}$ = 25.4, *C*O), 174.0 (t, $^2J_{CP}$ = 40.4, *NC*N), 134.8 (app. t, $^1J_{C-P}$ = 25.7, C_{ipso}), 131.5 (app. t, $^2J_{C-P}$ = 5.8, CH_{orto}), 131.2 (s, CH_{para}), 129.0 (app. t, $^3J_{C-P}$ = 5.0, CH_{meta}), 123.3 (s, CH_{im}), 46.4 (s, NCH_2), 29.1 (t, $^1J_{C-P}$ = 19.0, NCH_2). $^{31}P\{^1H\}$ NMR (CD_3CN, 121 MHz): δ 59.2 (s, PPh_2). IR (cm^{-1}, pure sample): 1932, 1882 cm^{-1}. HRMS (ESI+): *m*/*z* calcd for $C_{32}H_{30}N_2OP_2CoBF_4$: (M–CO–$Cl^-$): 579.1114, Exp: 579.1165.

General procedure for the catalytic reductive amination of furfural

To a Schlenk flask equipped with a magnetic stir bar, furfural (10 μL, 0.125 mmol), *p*-toluidine (13.4 mg, 0.125 mmol), 5 mol% of the catalyst **1** (3.9 mg, 0.0063 mmol) and 1 mL of DMC as solvent were added. The resulting solution was stirred at 80 °C for 1 h. Afterwards, 2 equivalents of $PhSiH_3$ (31 μL, 0.25 mmol) was added under argon and stirred again at 80 °C for 20 h. The resulting solution was evaporated under reduced pressure and the conversion was determined by ^1H NMR spectroscopy of the crude material in $CDCl_3$.[44]

General procedure for the catalytic reductive amination of levulinic acid

To a Schlenk flask equipped with a magnetic stir bar, levulinic acid (26 μL, 0.25 mmol), *p*-toluidine (26.8 mg, 0.25 mmol), 1 mol% of the catalyst **1** (3.9 mg, 0.0026 mmol) and 6 equiva-

lents of $PhSiH_3$ (185 μL, 1.5 mmol) were added under argon. To the mixture thus obtained, mesitylene (6 μL, 0.04 mmol) was added as an internal standard and the solution was stirred at 80 °C for 5 h. $CDCl_3$ was added to an aliquot and measured by ^1H NMR to determine the yield of the reaction.[45]

Synthesis of *N*-(furan-2-ylmethyl)-4-methylaniline. To a Schlenk flask equipped with a magnetic stir bar, furfural (168 μL, 2.0 mmol), *p*-toluidine (217 mg, 2.0 mmol), 5 mol% of the catalyst **1** (65 mg, 0.10 mmol) and 10 mL of DMC as solvent were added under argon. The resulting solution was stirred at 80 °C for 1 h. Afterwards, 2 equivalents of $PhSiH_3$ (500 μL, 4.0 mmol) was added under argon and stirred again at 80 °C for 24 h with a bubbler in a well-ventilated fume hood. The resulting solution was quenched by adding 20 mL of methanol and 20 mL of 2M NaOH and stirred for 3 h. Subsequently, 50 mL of water was added and the product was extracted with diethyl ether (3 × 15 mL). The combined organic layers were dried over anhydrous $MgSO_4$, filtered and concentrated under reduced pressure. The product was purified by automatic flash chromatography purification using a puriFlash™ system with an ethyl acetate/hexane (10 : 90) mixture. After the collection and concentration under reduced pressure, the resulting amber-yellow oil was obtained in 79% yield (296 mg, 1.58 mmol). The NMR spectra matched those previously reported in the literature.[42a]

Synthesis of 2-methyl-1-(*p*-tolyl)pyrrolidine. To a Schlenk flask equipped with a magnetic stir bar, levulinic acid (139 μL, 1.35 mmol), *p*-toluidine (145 mg, 1.35 mmol), 1 mol% of the catalyst **1** (8.7 mg, 0.013 mmol) and 6 equivalents of $PhSiH_3$ (1 mL, 8.10 mmol) were added under argon. The resulting solution was stirred at 80 °C for 5 h with a bubbler in a well-ventilated fume hood. The resulting solution was quenched by adding 10 mL of methanol and 10 mL of 2M NaOH and stirred for 3 h. Subsequently, 25 mL of water was added and, the product was extracted with diethyl ether (3 × 10 mL). The combined organic layers were dried over anhydrous $MgSO_4$, filtered and concentrated under reduced pressure. The product was obtained by automatic flash chromatography purification using a puriFlash™ system with an ethyl acetate/hexane (10 : 90) mixture. After the collection and concentration under reduced pressure, the resulting amber oil was obtained in 87% yield (207 mg, 1.18 mmol). The NMR spectra matched those previously reported in the literature.[45a]

Crystal structure determination of 1. X-ray diffraction data of **1** were collected on a D8 VENTURE Bruker diffractometer with Mo κα radiation (λ = 0.71073 Å). A single crystal was mounted on a MiTeGen support, coated with perfluoropolyether oil and cooled to 100(2) K with open-flow nitrogen gas. Data were collected using narrow-frame ω and ϕ scans. Diffracted intensities were integrated and corrected of absorption effects using a multi-scan method with SAINT[46] and SADABS[47] programs, included in the APEX4 package. Structures were solved with direct methods with SHELXS[48] and refined with the SHELXL[49] program, included in the OLEX2 program.[50]

Structural data for 1. $C_{33}H_{30}CoN_2O_2P_2{\cdot}C_4CoO_4{\cdot}2(C_4H_8O)$; Mr = 922.64; yellow plate, 0.050 × 0.080 × 0.230 mm^3; monoclinic $P2_1/n$; a = 9.4757(2) Å, b = 25.3042(6) Å, c = 18.1856(5) Å; β = 92.9650(10)°; V = 4354.61(18) $Å^3$, Z = 4, D_c = 1.407 g cm^{-3}; μ = 0.890 cm^{-1}; min. and max. absorption correction factors: 0.7019 and 0.7457, $2\theta_{max}$ = 56.558°; 94 620 reflections measured, 10 813 unique; R_{int} = 0.0516; number of data/restraint/parameters 10 813/0/532; R_1 = 0.0361 [9320 ref. with $I > 2\sigma(I)$], w$R(F^2)$ = 0.0954 (all data); largest difference peak 0.646 e·$Å^{-3}$.

Conflicts of interest

There are no conflicts to declare.

Acknowledgements

Grants RTI2018-099136-A-I00 and PID2021-126212OB-I00 MCIN/AEI/10.13039/501100011033 funded by "ERDF A way of making Europe", as well as E42_23R, are gratefully acknowledged. The authors would like to acknowledge the use of "Servicio General de Apoyo a la Investigación-SAI" at the Universidad de Zaragoza and at the ISQCH/CEQMA (CSIC).

References

1 P. Gallezot, *Chem. Soc. Rev.*, 2012, **41**, 1538–1558.
2 H. Clark, T. J. Farmer, L. Herrero-Davila and J. Sherwood, *Green Chem.*, 2016, **18**, 3914–3934.
3 (*a*) R. A. Sheldon, *J. R. Soc., Interface*, 2016, **13**, 20160087; (*b*) P. Anastas and N. Eghbali, *Chem. Soc. Rev.*, 2010, **39**, 301–312.
4 (*a*) R. M. Bullock, J. G. Chen, L. Gagliardi, P. J. Chirik, O. K. Farha, C. H. Hendon, C. W. Jones, J. A. Keith, J. Klosin, S. D. Minteer, R. H. Morris, A. T. Radosevich, T. B. Rauchfuss, N. A. Strotman, A. Vojvodic, T. R. Ward, J. Y. Yang and Y. Surendranath, *Science*, 2020, **369**, eabc3183; (*b*) M. Albrecht, R. Bedford and B. Plietker, *Organometallics*, 2014, **33**, 5619–5621; (*c*) P. Chirik and R. Morris, *Acc. Chem. Res.*, 2015, **48**, 2495–2495.
5 (*a*) P. Gandeepan and C.-H. Cheng, *Acc. Chem. Res.*, 2015, **48**, 1194–1206; (*b*) G. Cahiez and A. Moyeux, *Chem. Rev.*, 2010, **110**, 1435–1462; (*c*) B. Su, Z.-C. Cao and Z.-J. Shi, *Acc. Chem. Res.*, 2015, **48**, 886–896.
6 (*a*) S. W. Anferov, A. S. Filatov and J. S. Anderson, *ACS Catal.*, 2022, **12**(16), 9933–9943; (*b*) L. N. Mendelsohn, C. S. MacNeil, L. Tian, Y. Park, G. D. Scholes and P. J. Chirik, *ACS Catal.*, 2021, **11**, 1351–1360; (*c*) P. J. Chirik, *Acc. Chem. Res.*, 2015, **48**, 1687–1695; (*d*) V. Papa, J. R. Cabrero-Antonino, A. Spannenberg, K. Junge and M. Beller, *Catal. Sci. Technol.*, 2020, **10**, 6125–6137; (*e*) S. Lapointe, D. K. Pandey, J. M. Gallagher, J. Osborne, R. R. Fayzullin, E. Khaskin and J. R. Khusnutdinova, *Organometallics*, 2021, **40**(21), 3617–3626; (*f*) H. Alawisi, H. D. Arman and Z. J. Tonzetich, *Organometallics*, 2021,

40(8), 1062–1070; (*g*) T. P. Lin and J. C. Peters, *J. Am. Chem. Soc.*, 2014, **136**, 13672–13683.

7 (*a*) G. Zhang and S. K. Hanson, *Chem. Commun.*, 2013, **49**, 10151–10153; (*b*) S. Fu, N.-Y. Chen, X. Liu, Z. Shao, S.-P. Luo and Q. Liu, *J. Am. Chem. Soc.*, 2016, **138**, 8588–8594; (*c*) M. Pang, J.-Y. Chen, S. Zhang, R.-Z. Liao, C.-H. Tung and W. Wang, *Nat. Commun.*, 2020, **11**, 1249; (*d*) R. V. Jagadeesh, D. Banerjee, P. B. Arockiam, H. Junge, K. Junge, M.-M. Pohl, J. Radnik, A. Brückner and M. Beller, *Green Chem.*, 2015, **17**, 898–902; (*e*) W. Ai, R. Zhong, X. Liu and Q. Liu, *Chem. Rev.*, 2018, **119**, 2876–2953.

8 (*a*) C. Chen, M. B. Hecht, A. Kavara, W. W. Brennessel, B. Q. Mercado, D. J. Weix and P. L. Holland, *J. Am. Chem. Soc.*, 2015, **137**, 13244–13247; (*b*) W. J. Teo, C. Wang, Y. W. Tan and S. Ge, *Angew. Chem., Int. Ed.*, 2017, **56**, 4328–4332; (*c*) B. Raya, S. Biswas and T. V. RajanBabu, *ACS Catal.*, 2016, **6**, 6318–6323; (*d*) Y. Gao, L. Wang and L. Deng, *ACS Catal.*, 2018, **8**, 9637–9646.

9 Examples for the hydrosilylation of carbonyl compounds: (*a*) T. W. Lyons and M. Brookhart, *Chem. – Eur. J.*, 2013, **19**, 10124–10127; (*b*) Q. Niu, H. Sun, X. Li, H.-F. Klein and U. Flörke, *Organometallics*, 2013, **32**, 5235–5238; (*c*) Y. Li, J. A. Krause and H. Guan, *Organometallics*, 2018, **37**, 2147–2158; (*d*) Y. Li, J. A. Krause and H. Guan, *Organometallics*, 2020, **39**, 3721–3730; (*e*) K. Matsubara, T. Mitsuyama, S. Shin, M. Hori, R. Ishikawa and Y. Koga, *Organometallics*, 2021, **40**, 1379–1387.

10 (*a*) V. Kumar, U. Sharma, P. K. Verma, N. Kumar and B. Singh, *Adv. Synth. Catal.*, 2012, **354**, 870–878; (*b*) C. C. Bories, M. Barbazanges, E. Derat and M. Petit, *ACS Catal.*, 2021, **11**, 14262–14273; (*c*) K. Murugesan, Z. H. Wei, V. G. Chandrashekhar, H. Neumann, A. Spannenberg, H. J. Jiao, M. Beller and R. V. Jagadeesh, *Nat. Commun.*, 2019, **10**, 5443.

11 (*a*) L. Zhang, Z. Zuo, X. Leng and Z. A. Huang, *Angew. Chem., Int. Ed.*, 2014, **53**, 2696–2700; (*b*) L. Zhang, Z. Zuo, X. Wan and Z. Huang, *J. Am. Chem. Soc.*, 2014, **136**, 15501–15504; (*c*) J. Guo, B. Cheng, X. Shen and Z. Lu, *J. Am. Chem. Soc.*, 2017, **139**, 15316–15319.

12 (*a*) J. Sun and L. Deng, *ACS Catal.*, 2016, **6**, 290–300; (*b*) A. D. Ibrahim, S. W. Entsminger, L. Zhu and A. R. Fout, *ACS Catal.*, 2016, **6**, 3589–3593; (*c*) B. Raya, S. Biswas and T. V. Rajanbabu, *ACS Catal.*, 2016, **6**, 6318–6323; (*d*) B. Raya, S. Jing, V. Balasanthiran and T. V. Rajanbabu, *ACS Catal.*, 2017, **7**, 2275–2283; (*e*) M. L. Scheuermann, E. J. Johnson and P. J. Chirik, *Org. Lett.*, 2015, **17**, 2716–2719; (*f*) W. N. Palmer, T. Diao, I. Pappas and P. J. Chirik, *ACS Catal.*, 2015, **5**(2), 622–626; (*g*) J. V. Obligacion and P. J. Chirik, *J. Am. Chem. Soc.*, 2013, **135**(51), 19107–19110.

13 C. M. Boudreaux, D. Nugegoda, W. Yao, N. Le, N. C. Frey, Q. Li, F. Qu, M. Zeller, C. E. Webster, J. H. Delcamp and E. T. Papish, *ACS Catal.*, 2022, **12**, 8718–8728.

14 (*a*) Y. Gao, Q. Chen, X. Leng and L. Deng, *Dalton Trans.*, 2019, **48**, 9676–9683; (*b*) Z. Mo, Y. Li, H. Lee and L. Deng, *Organometallics*, 2011, **30**, 4687–4694; (*c*) Z. Mo, J. Xiao, Y. Gao and L. Deng, *J. Am. Chem. Soc.*, 2014, **136**, 17414–17417; (*d*) Y. Meng, Z. Mo, B. Wang, Y. Zhang, L. Deng and S. Gao, *Chem. Sci.*, 2015, **6**, 7156–7162; (*e*) Z. Mo, D. Chen, X. Leng and L. Deng, *Organometallics*, 2012, **31**, 7040–7043.

15 (*a*) Y. Liu and L. Deng, *J. Am. Chem. Soc.*, 2017, **139**, 1798–1801; (*b*) A. D. Ibrahim, K. Tokmic, M. R. Brennan, D. Kim, E. M. Matson, M. J. Nilges, J. A. Bertke and A. R. Fout, *Dalton Trans.*, 2016, **45**, 9805–9811.

16 S. Takebayashi and R. R. Fayzullin, *Organometallics*, 2021, **40**, 500–507.

17 (*a*) S. P. Nolan, *N-Heterocyclic, Carbenes in Synthesis*, Wiley-VCH, Weinheim, 2006; (*b*) S. S. Bera and M. Szostak, *ACS Catal.*, 2022, **12**, 3111–3137.

18 (*a*) R. Weingarten, W. C. Conner and G. W. Huber, *Energy Environ. Sci.*, 2012, **5**, 7559–7574; (*b*) P. J. Deuss, K. Barta and J. G. de Vries, *Catal. Sci. Technol.*, 2014, **4**, 1174–1196; (*c*) J. J. Bozell and G. R. Petersen, *Green Chem.*, 2010, **12**, 539–554; (*d*) Y. W. Tiong, C. L. Yap, S. Gan and W. S. P. Yap, *Ind. Eng. Chem. Res.*, 2018, **57**, 4749–4766; (*e*) Z. Sun and K. Barta, *Chem. Commun.*, 2018, **54**, 7725–7745; (*f*) P. Y. Dapsens, C. Mondelli and J. Pérez-Ramírez, *ACS Catal.*, 2012, **2**, 1487–1499; (*g*) R. J. Van Putten, J. C. van der Waal, E. De Jong, C. B. Rasrendra, H. J. Heeres and J. G. De Vries, *Chem. Rev.*, 2013, **113**, 1499–1597; (*h*) T. Werpy and G. R. Petersen, *Top Value Added Chemicals from Biomass, Volume I. Results of Screening for Potential Candidates from Sugars and Synthesis Gas*, U.S. Department of Energy; U.S. Government Printing Office, Washington, DC, 2004.

19 (*a*) J. He, L. Chen, S. Liu, K. Song, S. Yang and A. Riisager, *Green Chem.*, 2020, **22**, 6714–6747; (*b*) G. Liang, A. Wang, L. Li, G. Xu, N. Yan and T. Zhang, *Angew. Chem., Int. Ed.*, 2017, **56**, 3050–3054; (*c*) J. D. Vidal, M. J. Climent, P. Concepcion, A. Corma, S. Iborra and M. J. Sabater, *ACS Catal.*, 2015, **5**(10), 5812–5821; (*d*) J. J. Roylance and K.-S. Choi, *Green Chem.*, 2016, **18**, 5412–5417; (*e*) A. Cukalovic and C. V. Stevens, *Green Chem.*, 2010, **12**, 1201–1206; (*f*) G. Chieffi, M. Braun and D. Esposito, *ChemSusChem*, 2015, **8**, 3590–3594; (*g*) M. Chatterjee, T. Ishizaka and H. Kawanami, *Green Chem.*, 2016, **18**, 487–496; (*h*) P. D. Pham, P. Bertus and S. Legoupy, *Chem. Commun.*, 2009, 6207–6209.

20 W. Ai, R. Zhong, X. Liu and Q. Liu, *Chem. Rev.*, 2019, **119**, 2876–2953.

21 (*a*) Y. Wei, C. Wang, X. Jiang, D. Xue, J. Li and J. Xiao, *Chem. Commun.*, 2013, **49**, 5408–5410; (*b*) Z. Sun, J. Chen and T. Tu, *Green Chem.*, 2017, **19**, 789–794; (*c*) C. Wu, X. Luo, H. Zhang, X. Liu, G. Ji, Z. Liu and Z. Liu, *Green Chem.*, 2017, **19**, 3525–3529; (*d*) Y. B. Huang, J. J. Dai, X. J. Deng, Y. C. Qu, Q. X. Guo and Y. Fu, *ChemSusChem*, 2011, **4**, 1578–1581; (*e*) Z. Xu, P. Yan, H. Jiang, K. Liu and Z. C. Zhang, *Chin. J. Chem.*, 2017, **35**, 581–585; (*f*) S. Wang, H. Huang, C. Bruneau and C. Fischmeister, *ChemSusChem*, 2017, **10**, 4150–4154.

22 D. Wei, C. Netkaew and C. Darcel, *Adv. Synth. Catal.*, 2019, **361**, 1781–1786.

23 M. C. Fu, R. Shang, W. M. Cheng and Y. Fu, *Angew. Chem., Int. Ed.*, 2015, **54**, 9042–9046.

24 A. Luque-Gómez, S. García-Abellán, J. Munarriz, V. Polo, V. Passarelli and M. Iglesias, *Inorg. Chem.*, 2021, **60**, 15497–15508.

25 (*a*) T. F. C. Cruz, L. F. Veiros and P. T. Gomes, *Inorg. Chem.*, 2018, **57**, 14671–14685; (*b*) T. F. C. Cruz, P. S. Lopes, L. C. J. Pereira, L. F. Veiros and P. T. Gomes, *Inorg. Chem.*, 2018, **57**, 8146–8159.

26 D. Cremer and J. A. Pople, *J. Am. Chem. Soc.*, 1975, **97**, 1354–1358. Puckering parameters for the metallacycle Co(1)–P(1)–C(14)–C(15)–N(1)–C(1): q = 0.9340(14) Å, θ = 80.45(9)°, φ = 4.47(8)°, for Co(1)–P(2)–C(19)–C(18)–N(2)–C(1): q = 0.9433(13) Å, θ = 78.63(10)°, φ = 8.78(10)°.

27 (*a*) R. L. Hollingsworth, J. W. Beattie, A. Grass, P. D. Martin, S. Groysman and R. L. Lord, *Dalton Trans.*, 2018, **47**, 15353–15363; (*b*) H. Van Rensburg, R. P. Tooze, D. F. Foster and A. M. Z. Slawin, *Inorg. Chem.*, 2004, **43**, 2468–2470; (*c*) A. R. Manning, *J. Chem. Soc. A*, 1968, 1135.

28 (*a*) L. M. Guard, T. J. Hebden, D. E. Linn and D. M. Heinekey, *Organometallics*, 2017, **36**, 3104–3109; (*b*) V. M. Krishnan, H. D. Arman and Z. J. Tonzetich, *Dalton Trans.*, 2018, **47**, 1435–1441.

29 M. A. Kent, C. H. Woodall, M. F. Haddow, C. L. McMullin, P. G. Pringle and D. F. Wass, *Organometallics*, 2014, **33**(20), 5686–5692.

30 M. Azam Rasool, P. P. Pescarmona and I. F. J. Vankelecom, *ACS Sustainable Chem. Eng.*, 2019, **7**(16), 13774–13785.

31 Related complexes have been reported to adopt facial geometries: (*a*) P. L. Chiu and H. M. Lee, *Organometallics*, 2005, **24**, 1692–1702; (*b*) V. Tegethoff, T. Lübbering, C. Schulte to Brinke, B. Schirmer, J. Neugebauer and F. E. Hahn, *Organometallics*, 2021, **40**(5), 606–617.

32 A similar pattern has been described by H. M. Lee for the same ligand *fac*-Ru complex (ref. 31*a*) and by us for a similar PCP ligand that coordinates to Ir adopting a facial geometry: M. Iglesias, A. Iturmendi, P. J. Sanz Miguel, V. Polo, J. J. Pérez-Torrente and L. A. Oro, *Chem. Commun.*, 2015, **51**, 12431–12434.

33 For examples of catalysed acceptorless dehydrogenative coupling of the silanes see: (*a*) L. Rosenberg, C. W. Davis and J. Yao, *J. Am. Chem. Soc.*, 2001, **123**, 5120–5121; (*b*) D. Schmidt, T. Zell, T. Schaubc and U. Radius, *Dalton Trans.*, 2014, **43**, 10816–10827; (*c*) E. E. Smith, G. Du, P. E. Fanwick and M. M. Abu-Omar, *Organometallics*, 2010, **29**, 6527–6533; (*d*) F. G. Fontaine and D. Zargarian, *J. Am. Chem. Soc.*, 2004, **126**, 8786–8794; (*e*) M. Tanabe, A. Takahashi, T. Fukuta and K. Osakada, *Organometallics*, 2013, **32**, 1037–1043; (*f*) M. D. Spencer, Q. D. Shelby and G. S. Girolami, *J. Am. Chem. Soc.*, 2007, **129**, 1860–1861; (*g*) T. D. Tilley, *Acc. Chem. Res.*, 1993, **26**, 22–29; (*h*) J. Y. Corey, X. H. Zhu, T. C. Bedard and L. D. Lange, *Organometallics*, 1991, **10**, 924–935.

34 (*a*) L. Rosenberg, C. W. Davis and J. Yaob, *J. Am. Chem. Soc.*, 2001, **123**, 5120–5121; (*b*) F.-G. Fontaine and D. Zargarian, *J. Am. Chem. Soc.*, 2004, **126**, 8786–8794; (*c*) E. E. Smith, G. Du, P. E. Fanwick and M. M. Abu-Omar, *Organometallics*, 2010, **29**, 6527–6533; (*d*) D. Schmidt, T. Zell, T. Schaub and U. Radius, *Dalton Trans.*, 2014, **43**, 10816–10827; (*e*) M. Tanabe, A. Takahashi, T. Fukuta and K. Osakada, *Organometallics*, 2013, **32**, 1037–1043.

35 (*a*) T. J. Clark, K. Lee and I. Manners, *Chem. – Eur. J.*, 2006, **12**, 8634–8648; (*b*) R. Waterman, *Chem. Soc. Rev.*, 2013, **42**, 5629–5641; (*c*) T. D. Tilley, *Acc. Chem. Res.*, 1993, **26**, 22–29.

36 (*a*) D. J. Parks and W. E. Piers, *J. Am. Chem. Soc.*, 1996, **118**, 9440–9441; (*b*) D. J. Parks, J. M. Blackwell and W. E. Piers, *J. Org. Chem.*, 2000, **65**, 3090–3098.

37 S. Park and M. Brookhart, *Organometallics*, 2010, **29**, 6057–6064.

38 V. K. Dioumaev and R. M. Bullock, *Nature*, 2003, **424**, 530–5352.

39 (*a*) J. Yang and M. Brookhart, *J. Am. Chem. Soc.*, 2007, **129**, 12656–12657; (*b*) S. Park and M. Brookhart, *J. Am. Chem. Soc.*, 2012, **134**, 640–653; (*c*) J. Yang, P. S. White, C. K. Schauer and M. Brookhart, *Angew. Chem., Int. Ed.*, 2008, **47**, 4141–4143.

40 (*a*) D. V. Gutsulyak, S. F. Vyboishchikov and G. I. Nikonov, *J. Am. Chem. Soc.*, 2010, **132**, 5950–5951; (*b*) D. V. Gutsulyak and G. I. Nikonov, *Angew. Chem., Int. Ed.*, 2010, **49**, 7553–7556; (*c*) D. V. Gutsulyak, A. van der Est and G. I. Nikonov, *Angew. Chem., Int. Ed.*, 2011, **50**, 1384–1387; (*d*) S.-H. Lee, D. V. Gutsulyak and G. I. Nikonov, *Organometallics*, 2013, **32**, 4457–4464.

41 (*a*) T. T. Metsänen, D. Gallego, T. Szilvási, M. Driess and M. Oestreich, *Chem. Sci.*, 2015, **6**, 7143–7149; (*b*) J. Fuchs, H. F. T. Klare and M. Oestreich, *ACS Catal.*, 2017, **7**, 8338–8342; (*c*) S. Rendler and M. Oestreich, *Angew. Chem., Int. Ed.*, 2008, **47**, 5997–6000.

42 (*a*) M. Iglesias, P. J. Sanz Miguel, V. Polo, F. J. Fernández-Alvarez, J. J. Pérez-Torrente and L. A. Oro, *Chem. – Eur. J.*, 2013, **19**, 17559–17566; (*b*) R. Lalrempuia, M. Iglesias, V. Polo, P. J. Sanz Miguel, F. J. Fernández-Alvarez, J. J. Pérez-Torrente and L. A. Oro, *Angew. Chem., Int. Ed.*, 2012, **51**, 12824–12827; (*c*) R. Puerta-Oteo, J. Munarriz, V. Polo, M. V. Jiménez and J. J. Pérez-Torrente, *ACS Catal.*, 2020, **10**(13), 7367–7380.

43 (*a*) Y. D. Y. L. Getzler, V. Mahadevan, E. B. Lobkovsky and G. W. Coates, *J. Am. Chem. Soc.*, 2002, **124**, 1174–1175; (*b*) J. A. R. Schmidt, E. B. Lobkovsky and G. W. Coates, *J. Am. Chem. Soc.*, 2005, **127**, 11426–11435; (*c*) T. L. Church, Y. D. Y. L. Getzler and G. W. Coates, *J. Am. Chem. Soc.*, 2006, **128**, 10125–10133; (*d*) J. M. Rowley, E. B. Lobkovsky and G. W. Coates, *J. Am. Chem. Soc.*, 2007, **129**, 4948–4960; (*e*) Y. Wen, R. Nie, B. Li and S. Li, *ACS Catal.*, 2023, **13**, 3317–3322.

44 The products of the reductive amination of furfural have been previously reported in the literature.(*a*) *N*-(Furan-2-ylmethyl)-4-methylaniline: D. Weickmann, W. Frey and B. Plietker, *Chem. – Eur. J.*, 2013, **19**, 2741–2748; (*b*) *N*-(Furan-2-ylmethyl)aniline: P. D. Pham, P. Bertus and S. Legoupy, *Chem. Commun.*, 2009, 6207–6209; (*c*) *N*-(Furan-2-ylmethyl)-4-methoxyaniline: J. S. K. Clark, C. M. Lavoie,

P. M. MacQueen, M. J. Ferguson and M. Stradiotto, *Organometallics*, 2016, **35**, 3248–3254; (*d*) *N*-(Furan-2-ylmethyl)-4-(trifluoromethyl)aniline: Y. Du, R. M. Pearson, C.-H. Lim, S. M. Sartor, M. D. Ryan, H. Yang, N. H. Damrauer and G. M. Miyake, *Chem. – Eur. J.*, 2017, **23**, 10962–10968; (*e*) *N*-(Furan-2-ylmethyl)cyclohexanamine: C. D. Matier, J. Schwaben, J. C. Peters and G. C. Fu, *J. Am. Chem. Soc.*, 2017, **139**, 17707–17710; (*f*) 4-(Furan-2-ylmethyl)morpholine: Z. Şahin, N. Gürbüz, İ. özdemir, O. Şahin, O. Büyükgüngör, M. Achard and C. Bruneau, *Organometallics*, 2015, **34**, 2296–2304.

45 The products of the reductive amination of levulinic acid. 2-methyl-1-(*p*-tolyl)pyrrolidine, phenylpyrrolidine: (*a*) 2-Methyl-1- has been previously reported in the literatureY. Ogiwara, T. Uchiyama and N. Sakai, *Angew. Chem., Int. Ed.*, 2016, **55**, 1864–1867; (*b*) 1-(4-Methoxyphenyl)-2-methylpyrrolidine: Y. Zhang, X. Yang, Q. Yao and D. Ma, *Org. Lett.*, 2012, **14**, 3056–3059; (*c*) 2-Methyl-1-(4-(trifluoromethyl)phenyl)pyrrolidine: C. Li, Y. Kawamata, H. Nakamura, J. C. Vantourout, Z. Liu, Q. Hou, D. Bao, J. T. Starr, J. Chen, M. Yan and P. S. Baran, *Angew. Chem., Int. Ed.*, 2017, **56**, 13088–13093; (*d*) C. Wu, X. Luo, H. Zhang, X. Liu, G. Ji, Z. Liu and Z. Liu, *Green Chem.*, 2017, **19**, 3525–3529.

46 *SAINT+, version 6.01: Area-Detector Integration Software*, Bruker AXS, Madison, WI, 2001.

47 SADABS, *Area-Detector Absorption Program*, Bruker AXS, Madison, WI, 1996; L. Krause, R. Herbst-Irmer, G. M. Sheldrick and D. Stalke, *J. Appl. Crystallogr.*, 2015, **48**, 3–10.

48 G. M. Sheldrick, *Acta Crystallogr.*, 2008, **A64**, 112–122.

49 G. M. Sheldrick, *Acta Crystallogr.*, 2015, **A71**, 3–8.

50 O. V. Dolomanov, L. J. Bourhis, R. J. Gildea, J. A. K. Howard and H. Puschmann, *J. Appl. Crystallogr.*, 2009, **42**, 339–341.